8.5 (SD) for the right-handers and -10 for the ambidextrous participant.
12. Rest was as defined [P. E. Roland and B. Larsen, *Arch. Neurol.* **33**, 551 (1976)]. The arterial partial pressure of CO_2 and O_2 was measured repetitively, and the EEG and electrooculogram (EOG) were recorded continuously. None of the participants broke their fixated gazes, and the EOG showed only eye blinks with an average frequency of 0.2 ± 0.1 Hz (mean ± SD). The background illumination was 0.27 cd/m^2 during all conditions.
13. The visual stimulus for fixation was a 3° visual angle yellow monochrome circle 0.8 cd/m^2 on a monitor. At random intervals ranging from 1000 to 3000 ms, the luminance of the circle suddenly increased to 14.5 cd/m^2 for 1000 ms.
14. Experiment participants during all conditions rested the pad of the right index finger on a polyvinyl plate having an 11-mm-diameter hole through which a 2-mm stylus driven by a solenoid could protrude. The stylus did not touch the skin in the interstimulus intervals. The interstimulus intervals ranged from 1000 to 3000 ms in a random manner. In the somatosensory task, the stylus indented the pulp of the index finger by 2.8 mm for 1000 ms.
15. The visual reaction time was 315 ± 39 ms (mean ± SD); the somatosensory reaction time was 288 ± 29 ms. The global blood flow of the brain increased from 46.1 ± 5.3 ml/100 g/min at rest to 49.5 ± 4.6 ml/100 g/min and 50.5 ± 4.9 ml/100 g/min in the vis-RT and som-RT tasks, respectively. The percentage α-blockade in the EEG was 80.1 ± 17.2 (mean ± SD) during rest and 80.1 ± 20.1 during the som-RT task but increased to 90.7 ± 8.2 during the vis-RT task ($P < 0.01$; *t* test). Heart rate did not change significantly [62.0 ± 6.0 beats/min (rest), 62.8 ± 6.6 beats/min (vis-RT), and 63.2 ± 6.7 beats/min (som-RT)]; neither did the arterial CO_2 pressure [5.59 ± 0.23 kPa (rest), 5.56 ± 0.23 kPa (vis-RT), and 5.62 ± 0.33 kPa (som-RT)].
16. The accuracy (SEM) of localizing structures in the upper brainstem in PET and magnetic resonance images was <0.35 mm. The center of gravity of the right red nucleus was determined in the brainstem in each participant (*23*). In the anatomically standardized format, the mean coordinates ± SEM for the 10 participants were *x* (medio-lateral), 5.16 ± 0.19 mm; *y* (anterior-posterior), 18.90 ± 0.31 mm; and *z* (superior-inferior), 6.86 ± 0.19 mm.
17. G. Schaltenbrand and P. Bailey, *Einführung in die Stereo-taktischen Operationen mit einem Atlas des menschlichen Gehirns* (Thieme Verlag, Stuttgart, 1959).
18. The rCBFs in the right and left midbrain tegmentum were 54.9 ± 4.9 ml/100 g/min and 53.5 ± 4.9 ml/100 g/min, respectively, for the som-RT (mean ± SEM); for the vis-RT task, the corresponding values were 54.7 ± 5.3 and 53.9 ± 5.6 ml/100 g/min, respectively. For the right and left intralaminar nuclei of the thalamus, the rCBFs were 64.5 ± 4.3 ml/100 g/min and 69.7 ± 6.3 ml/100 g/min, respectively, for the som-RT, and 74.9 ± 4.4 ml/100 g/min and 68.6 ± 6.5 ml/100 g/min, respectively, for the vis-RT task. For comparison, a ROI (region of interest) symmetrical to the activated part was drawn.
19. The experiment participants were nine normal male volunteers aged 23 to 29 years, eight of whom were right-handed and one of whom was left-handed. In the task, they were trained for 10 min to produce a rate acceptably close to the stipulated 0.33 Hz. The luminance of the homogenous yellow light on the screen was 4.2 cd/m^2. The color coordinates were $x = 0.51$ and $y = 0.426$ (Commission International d'Éclairage). The procedures and PET measurements were identical to those made in the reaction-time group. The global rCBF was 46.6 ± 5.4 ml/100 g/min. The α-blockade was 79.3 ± 16.5%, the frequencies of eye blinks 0.3 ± 0.1 Hz, and the arterial CO_2 pressure 5.56 ± 0.24 kPa, all of which were similar to the values obtained in the rest and RT conditions. Specifically, there were no differences in the frequency of thumb movements in the RT conditions and the self-generated movement condition, values for which were as follows: 0.35 ± 0.01 Hz (vis-RT), 0.31 ± 0.02 Hz (som-RT), and 0.29 ± 0.06 Hz (self-generated thumb movements). Other procedures were as described (*9*).
20. J. Decety, R. Kawashima, B. Gulyás, P. E. Roland, *NeuroReport* **3**, 761 (1992); B. T. O'Sullivan, P. E. Roland, R. Kawashima, *Eur. J. Neurosci.* **6**, 137 (1994); R. Kawashima, B. T. O'Sullivan, P. E. Roland, *Cerebr. Cortex* **2**, 111 (1995).
21. S. S. Kety, *Am. J. Med.* **8**, 205 (1950); D. Ingvar *et al.*, *Arch. Neurol.* **11**, 13 (1964); P. E. Roland, L. Eriksson, S. Stone-Elander, L. Widén, *J. Neurosci.* **7**, 2373 (1987); P. E. Roland, *Brain Activation* (Wiley, New York, 1993).
22. P. E. Roland *et al.*, *Human Brain Mapping* **1**, 3 (1993).
23. P. E. Roland *et al.*, *ibid.* **1**, 173 (1994).
24. The vca plane, which is tangent to the anterior commissure, defines the zero coordinate in the the anterior-posterior axis (Table 1). The vcp plane is vertical tangent to the posterior commissure. The ac-pc (commissural) plane defines the zero coordinate in the superior-inferior axis.
25. Supported by the Human Capital and Mobility Programme of the European Commission and the Swedish Medical Research Council. We thank J. Pedersen and W. Pulka for technical assistance.

6 June 1995; accepted 21 November 1995

Altered Reactivity of Superoxide Dismutase in Familial Amyotrophic Lateral Sclerosis

Martina Wiedau-Pazos,* Joy J. Goto,* Shahrooz Rabizadeh, Edith B. Gralla, James A. Roe, Michael K. Lee, Joan S. Valentine,† Dale E. Bredesen†

A subset of individuals with familial amyotrophic lateral sclerosis (FALS) possesses dominantly inherited mutations in the gene that encodes copper-zinc superoxide dismutase (CuZnSOD). A4V and G93A, two of the mutant enzymes associated with FALS, were shown to catalyze the oxidation of a model substrate (spin trap 5,5′-dimethyl-1-pyrroline *N*-oxide) by hydrogen peroxide at a higher rate than that seen with the wild-type enzyme. Catalysis of this reaction by A4V and G93A was more sensitive to inhibition by the copper chelators diethyldithiocarbamate and penicillamine than was catalysis by wild-type CuZnSOD. The same two chelators reversed the apoptosis-inducing effect of mutant enzymes expressed in a neural cell line. These results suggest that oxidative reactions catalyzed by mutant CuZnSOD enzymes initiate the neuropathologic changes in FALS.

Amyotrophic lateral sclerosis (ALS), or Lou Gehrig's disease, is a motor neuron degenerative disease that affects approximately 1 person in 10,000. About 10 to 15% of cases are familial (*1*), and 20 to 25% of familial ALS (FALS) cases are associated with dominantly inherited mutations in *SOD1*, the gene that encodes human CuZnSOD (*2*). Initial studies of the FALS-associated CuZnSOD mutants appeared to demonstrate reduced enzymatic activity (*3*). However, subsequent studies with transgenic mouse (*4*) and cell culture (*5*) models of FALS indicated a dominant, gain-of-function effect of the FALS-associated CuZnSOD mutants. Moreover, yeast *sod1* null mutants were rescued as efficiently by FALS-associated mutant human CuZnSOD as by the wild-type (WT) human enzyme, which indicated extensive activity of the mutant proteins (*5*). Although these observations supported a gain-of-function effect of the mutants, the nature of the function gained has remained undetermined (*1*).

In addition to its activity as a SOD (*6*), CuZnSOD catalyzes oxidation of substrates by hydrogen peroxide (H_2O_2) at rates competitive with its own oxidative inactivation by the same reagent (*7*, *8*). A convenient substrate used to study this type of reaction is the spin trap 5,5′-dimethyl-1-pyrroline *N*-oxide (DMPO), which reacts with H_2O_2 to give its electron paramagnetic resonance (EPR)–detectable hydroxyl adduct, DMPO-OH, in a reaction catalyzed by WT CuZnSOD (*9*). We hypothesized that the FALS-associated mutant CuZnSODs might enhance similar oxidative reactions of substrates with H_2O_2 because the locations of the FALS-associated mutations in this enzyme suggest the possibility of increased openness of the three-dimensional structures (*3*), which could conceivably allow greater access of substrates to the active site. In addition, in a neuronal cell culture model of FALS, mutant human CuZnSODs [Ala^4 → Val (A4V) and Gly^{37} → Arg (G37R)] increased apoptosis, whereas the

M. Wiedau-Pazos, J. J. Goto, E. B. Gralla, J. S. Valentine, Department of Chemistry and Biochemistry, University of California, Los Angeles, CA 90095, USA.
S. Rabizadeh, Interdepartmental Program for Neuroscience, University of California, Los Angeles, CA 90095, USA, and Program on Aging, La Jolla Cancer Research Foundation, La Jolla, CA 92037, USA.
J. A. Roe, Department of Chemistry and Biochemistry, Loyola Marymount University, Los Angeles, CA 90045, USA.
M. K. Lee, Department of Pathology, Johns Hopkins University School of Medicine, Baltimore, MD 21218, USA.
D. E. Bredesen, Program on Aging, La Jolla Cancer Research Foundation, La Jolla, CA 92037, USA.

*These authors contributed equally to this report.
†To whom correspondence should be addressed.

WT human CuZnSOD inhibited apoptosis (*5*, *10*), and apoptosis has been demonstrated in some instances to be mediated by reactive oxygen species (*11*).

To test the hypothesis that FALS-associated mutations augment the catalytic oxidation of substrates by H_2O_2, we expressed recombinant WT and mutant proteins A4V and G93A ($Gly^{93} \rightarrow Ala$) in the yeast *Saccharomyces cerevisiae* and purified them to homogeneity (*6*, *12*). EPR studies were performed with H_2O_2 and DMPO (*9*). Solutions containing fully metallized mutant or WT enzymes produced the quadruplet signal characteristic of DMPO-OH (*13*) when both H_2O_2 and DMPO were present (Fig. 1). Double integration of the signals attributable to the adduct demonstrated that significantly higher concentrations of DMPO-OH were generated with the FALS-associated mutant enzymes. The amplitude of the signal generated by the A4V mutant was reproducibly greater than that obtained with the G93A mutant, which in turn was reproducibly greater than that obtained with WT CuZnSOD (*14*). The apoenzymes did not produce detectable amounts of DMPO-OH (Fig. 2). With increasing extents of metallation by Cu^{2+}, however, the enzymes generated increasing DMPO-OH signals (Fig. 2). Differences between WT and mutant enzymes were apparent at all degrees of metallation. The increase in the EPR signals was not simply attributable to free Cu^{2+} in solution, because free Cu^{2+} without enzyme did not generate a significant DMPO-OH signal (Fig. 1).

Previous studies of the oxidation of substrates by H_2O_2 catalyzed by WT CuZnSOD suggested that the reaction occurs at the Cu^{2+} ion bound at the active site of each subunit of the enzyme (*7*–*9*). We therefore investigated the effect of adding Cu^{2+}-chelating agents, either diethyldithiocarbamate (DDC) (*15*) or *d*,*l*-penicillamine (*16*), to the reaction system. The WT enzyme showed a small concentration-dependent increase in DMPO-OH production after the addition of small amounts of DDC (Fig. 3). In contrast, both A4V and G93A showed a progressive decrease in DMPO-OH generation with increasing concentrations of DDC. A concentration-dependent decrease in DMPO-OH production was observed for both WT and A4V enzymes (G93A was not studied) on addition of penicillamine (*17*).

The results of the DDC and penicillamine experiments did not discriminate between the possibility that these reagents remove Cu^{2+} from the active site of the mutant enzymes and the alternative possibility that they bind to the Cu^{2+} and thus inhibit its reaction with H_2O_2, DMPO, or both (*18*). Previous observations (*15*) indicate that, at low concentrations, DDC binds to WT bovine CuZnSOD without inhibiting its SOD activity. Similar studies with penicillamine and WT CuZnSOD have not been reported. Nevertheless, the observation that each of these Cu^{2+} chelators interferes with the ability of the mutant CuZnSOD enzymes to catalyze production of DMPO-OH implies that the Cu^{2+} in each enzyme participates in the catalytic mechanism.

We reasoned that if similar oxidative reactions catalyzed by mutant CuZnSODs are important in SOD-associated FALS, then Cu^{2+} chelators might likewise inhibit the process of neural degeneration in our neural cell culture model of FALS, in which overexpression of WT CuZnSOD inhibits apoptosis whereas similar levels of expression of FALS-associated mutant CuZnSODs enhance apoptosis (*5*). The neural cell line CSM14.1 (*19*) was transfected with expression constructs encoding WT human CuZnSOD or the mutant human CuZnSODs A4V, G37R, G41D ($Gly^{41} \rightarrow Asp$), or G85R ($Gly^{85} \rightarrow Arg$). Overexpression of the WT CuZnSOD inhibited apoptosis induced in the cells by serum withdrawal, whereas all four mutants tested enhanced apoptosis relative to the control (*5*). DDC (25 to 100 μM) inhibited by 30 to 70% apoptosis induced by all four mutants, but had no effect on cells overexpressing WT CuZnSOD (Fig. 4). At a concentration of 500 μM, DDC decreased the viability of cells expressing WT CuZnSOD but continued to rescue the cells expressing the mutant CuZnSODs. At a concentration of ≥1 mM, DDC was toxic in all groups. Similar results were obtained with penicillamine (*20*).

Our EPR results indicate that two FALS-associated CuZnSOD mutants catalyze the reaction of H_2O_2 with DMPO to produce substantially higher amounts of DMPO-OH than those produced with the WT enzyme. The observations that Cu^{2+} chelators inhibit this DMPO-OH production and increase the viability of cultured neural cells expressing each of four FALS-associated CuZnSOD mutants suggest that such mutant enzymes may similarly catalyze

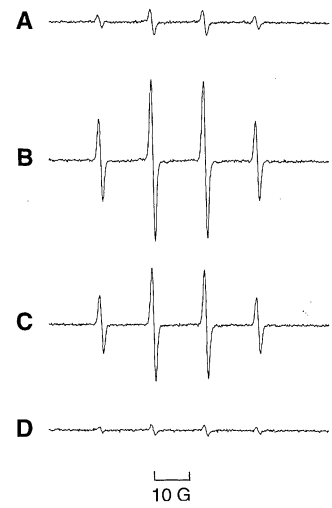

Fig. 1. EPR spectra of the DMPO-OH adduct formed in the presence of human WT CuZnSOD, mutant CuZnSODs, and Cu^{2+}. (**A**) WT enzyme, (**B**) A4V mutant, (**C**) G93A mutant, and (**D**) copper(II) sulfate. The signals shown are representative; measurements of mutant enzyme were repeated 5 to 10 times, always paired with the WT protein. Reactions were performed as described (*9*), with minor modifications: Reaction mixtures consisted of 1.25 μM protein (or 2.5 μM $CuSO_4$) and 45 mM DMPO (Aldrich) in 23.5 mM $NaHCO_3$ buffer (pH 7.4) balanced with 5% CO_2 and 95% N_2. The reaction was initiated by injection of 30 mM H_2O_2. Spectra developed after 30 to 45 s, were recorded at 5 min, and were stable for > 30 min. EPR spectra were recorded at room temperature on a Bruker ER 200 D instrument, operated at 9.5 GHz with a modulation frequency of 100 kHz. Conditions were as follows: microwave power, 20.7 mW; modulation amplitude, 1 G; time constant, 10 ms; sweep width, 100 G with 2046-point resolution. The samples were prepared and handled, and all measurements executed, in a strictly oxygen-free atmosphere to prevent radical scavenging by molecular oxygen. Buffers were treated with Chelex 100 (Bio-Rad) to eliminate the possibility of contamination by trace metals. DMPO was purified by filtration with neutral decolorizing charcoal (Aldrich) (*25*). The concentration of DMPO was calibrated spectrophotometrically, with an extinction coefficient at 226 nm of $7.22 \times 10^3\ M^{-1}\ cm^{-1}$ (*26*). An aqueous flat cell (Wilmad) was used to hold the samples. The concentrations of the apoproteins were calculated from an extinction coefficient at 280 nm of $1.08 \times 10^4\ M^{-1}\ cm^{-1}$.

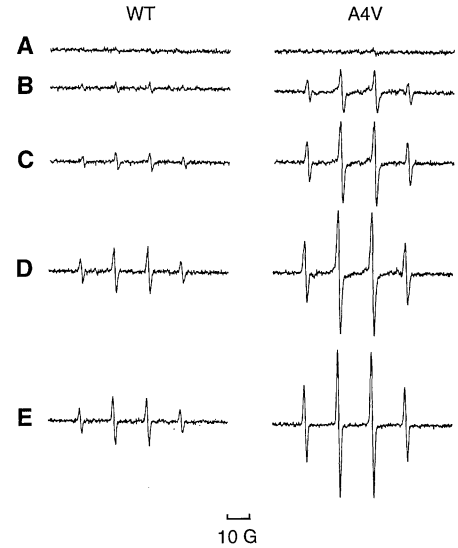

Fig. 2. EPR spectra of the DMPO-OH adduct formed in the presence of human WT CuZnSOD and mutant A4V at different extents of copper metallation of the proteins. (All samples contained one equivalent of zinc per subunit.) (**A**) Copper-free enzyme; (**B** through **E**) WT (left traces) and mutant (right traces) enzymes with 25, 50, 75, and 100% copper metallation, respectively. Experiments were performed as described in Fig. 1 and were repeated three times. Representative signals, recorded at 3 min, are shown.

oxidation of substrates present in motor neurons. H_2O_2 need not necessarily be the primary oxidant in such mutant CuZnSOD–catalyzed reactions, because alternative oxidants, such as peroxynitrite (*21*) or organic peroxides, may act in a similar manner. In addition, in our EPR experimental system, H_2O_2 acts both as a reductant of the Cu(II) form of the enzyme and as an oxidant of DMPO (*22*), whereas intracellular reducing agents may act as reductants of the Cu(II) form of the enzyme in motor neurons. Thus, oxidative reactions of H_2O_2 may occur in motor neurons at lower concentrations of this compound than those used in our in vitro studies.

In any event, the most important difference between the in vitro and in vivo systems is that, whereas DMPO is the substrate in vitro, the target substrates in motor neurons are unknown. Potential candidates for such substrates include small anionic molecules, such as formate or glutamate, that may fit into the active site channel and be oxidized at the active site. Likely products of such reactions are formyl or glutamyl radicals, which in turn may participate in longer range oxidative reactions. Indeed, the ability of glutamate to prevent the inactivation of WT CuZnSOD by reacting with H_2O_2 within the active site channel has been attributed to such a mechanism (*9*). Identification of substrates whose oxidation is catalyzed by mutant CuZnSOD enzymes in motor neurons may provide clues to other causes of familial and sporadic ALS. Our observation that Cu^{2+} chelators inhibit the ability of mutant CuZnSOD enzymes both to catalyze oxidation of substrates by H_2O_2 in vitro and to induce apoptosis in cell culture suggests that such agents, although potentially toxic (*16*, *23*), should be tested in animal models of FALS (*4*), with the hope that they may ultimately be beneficial in patients with FALS associated with *SOD1* mutations.

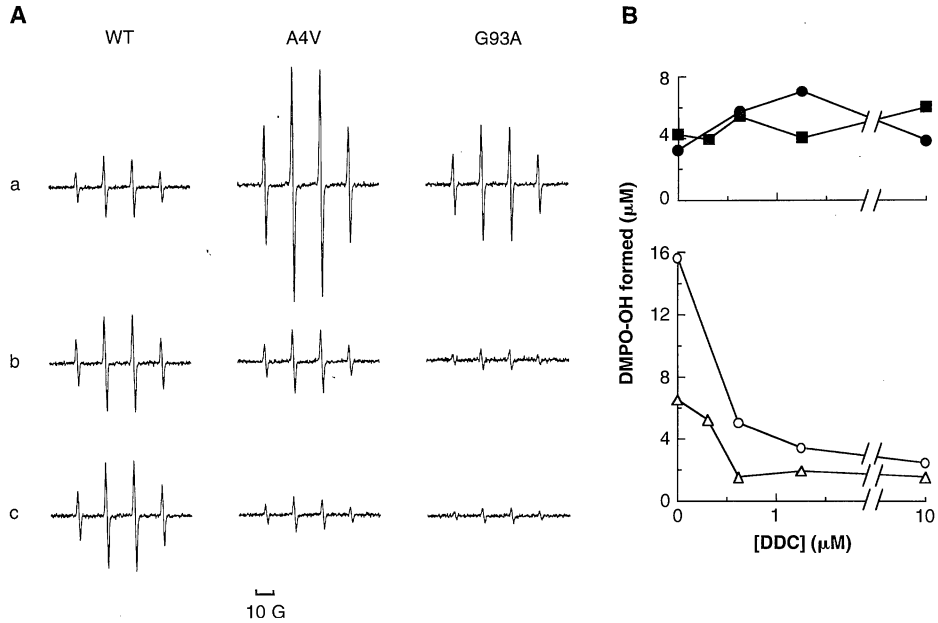

Fig. 3. (**A**) EPR spectra of the DMPO-OH adducts formed by human WT (left traces), A4V (middle traces), and G93A (right traces) CuZnSOD with various concentrations of DDC: (a) No DDC added; (b) 0.62 μM DDC; and (c) 10 μM DDC. Experiments were performed as in Fig. 1 and were repeated two or three times. DDC was prepared freshly and added to the CuZnSOD immediately before addition of DMPO and injection of H_2O_2. Spectra were recorded at 2.5 min. (**B**) Concentrations of DMPO-OH formed during the reaction of H_2O_2 (30 mM) with WT (■ and ●, which represent two separate series of experiments), A4V (○), and G93A (△) CuZnSOD in the presence of various concentrations of DDC. Reaction conditions were as in Fig. 1. Experiments were repeated two or three times. The concentrations were determined by double integration of the DMPO-OH EPR signals with the spin label carbamoyl-proxyl (Aldrich) as a standard.

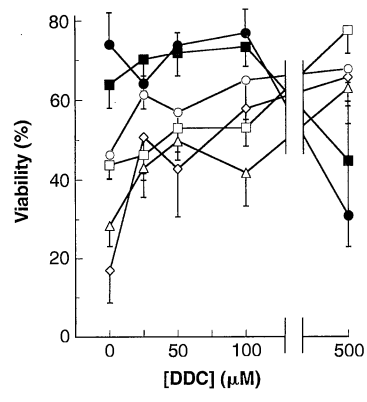

Fig. 4. Effect of DDC on serum withdrawal–induced apoptosis of temperature-sensitive nigral neural cells (CSM14.1) expressing WT or mutant CuZnSOD. Cells were transfected with the vector only (■), the WT gene (●), or A4V (△), G37R (◇), G41D (□), or G85R (○) mutant SOD constructs (*5*). After selection in puromycin (7 μg/ml), cells were transferred to 96-well plates and incubated in serum-free medium containing various concentrations of DDC. Viability was assessed after 60 hours (*5*). There was no significant improvement in viability at any DDC concentration for cells transfected with the WT construct. In contrast, cells transfected with mutant SODs showed significant improvements in survival. Analysis by unpaired two-tailed *t* test showed the following: For A4V and G37R, $P < 0.01$; for G85R, $P < 0.01$ (except at 50 μM, where $P < 0.05$); for G41D, $P < 0.05$ at 50 and 100 μM and $P < 0.01$ at 500 μM. Data are means ± SEM of four experiments.

REFERENCES AND NOTES

1. R. H. Brown Jr., *Cell* **80**, 687 (1995).
2. D. R. Rosen *et al.*, *Nature* **362**, 59 (1993).
3. H. X. Deng *et al.*, *Science* **261**, 1047 (1993).
4. M. E. Gurney *et al.*, *ibid.* **264**, 1772 (1994); M. E. Ripps, G. W. Huntley, P. R. Hof, J. H. Morrison, J. W. Gordon, *Proc. Natl. Acad. Sci. U.S.A.* **92**, 689 (1995); C. A. Pardo *et al.*, *ibid.*, p. 954.
5. S. Rabizadeh *et al.*, *Proc. Natl. Acad. Sci. U.S.A.* **92**, 3024 (1995).
6. J. M. McCord and I. Fridovich, *J. Biol. Chem.* **244**, 6049 (1969); I. Fridovich, *Annu. Rev. Biochem.* **64**, 97 (1995).
7. E. K. Hodgson and I. Fridovich, *Biochemistry* **14**, 5294 (1975); *ibid.*, p. 5299.
8. D. E. Cabelli, D. Allen, B. H. J. Bielski, *J. Biol. Chem.* **264**, 9967 (1989).
9. M. B. Yim, P. B. Chock, E. R. Stadtman, *Proc. Natl. Acad. Sci. U.S.A.* **87**, 5006 (1990); *J. Biol. Chem.* **268**, 4099 (1993).
10. L. J. S. Greenlund, T. L. Deckwerth, E. M. Johnson Jr., *Neuron* **14**, 303 (1995).
11. T. A Sarafian and D. E. Bredesen, *Free Radical Res.* **21**, 1 (1994).
12. Complementary DNA clones for human WT CuZnSOD and the A4V and G93A mutants, under the control of the yeast *SOD1* promoter, were cloned into the yeast shuttle vector YEp351 and transformed into yeast strain EG118, which is null for yeast *SOD1* (*5*). Cultures of 10 liters were grown in highly aerated YEPD medium (5% yeast extract, 10% peptone, and 2% dextrose) for 24 hours. Cells were harvested by centrifugation, resuspended in a small volume, and lysed with an equal volume of 0.5-mm glass beads in a blender. Protein purification was as described [Y. Lu *et al.*, *J. Am. Chem. Soc.* **115**, 5907 (1993)], with the addition of a final Sephadex G75 (Pharmacia) chromatography step. The purified proteins were homogeneous, as indicated by SDS–polyacrylamide gel electrophoresis. For each batch, 50 to 200 mg of purified protein was obtained. Human CuZnSOD expressed in yeast is acetylated normally at the NH_2-terminus [R. A. Hallewell *et al.*, *Biotechnology* **5**, 363 (1987)]. The identities of the purified mutant proteins were verified by electrospray mass spectrometry, which detected the change in mass attributable to single amino acid substitutions. For both WT and mutant proteins, the observed and predicted masses corresponded, within 2 to 4 atomic mass units. Copper and zinc ions were removed and the apoenzymes were recombined with metal by the gradual addition of $CuSO_4$ and $ZnSO_4$ [C. R. Nishida, E. B. Gralla, J. S. Valentine, *Proc. Natl. Acad. Sci. U.S.A.* **91**, 9906 (1994)]. The extent of metallation was confirmed by atomic absorption spectrometry. The specific activities of the mutant enzymes were determined with the 6-hydroxydopamine assay (*24*) and were shown to be 96% for A4V and 75% for G93A, relative to the human WT enzyme.
13. Assignment of this signal to DMPO-OH was based on its typical A-B-B-A quadruplet pattern and its hyperfine coupling constant of 14.9 G (*9*). We also performed similar reactions but with addition of ethanol (2.3 or 3.1 M) and observed a small signal attributable to the hydroxyethyl adduct of DMPO in addition to the large signal attributable to DMPO-OH

[L. A. Reinke, D. R. Moore, C. M. Hague, P. B. McCay, *Free Radical Res.* **21**, 213 (1994)].
14. The signal attributable to DMPO-OH for A4V was 3.0 ± 1.1 times the WT signal (mean ± SEM, $n = 10$, $P < 0.005$ by unpaired, two-tailed t test; range, 2.1 to 5.7 times the WT signal), and that attributable to G93A was 2.1 ± 0.3 times the WT signal ($n = 5$, $P < 0.025$, range, 1.8 to 2.6 times the WT signal). Studies were also performed with WT and A4V enzymes at lower concentrations of H_2O_2. Marked DMPO-OH signals were observed at H_2O_2 concentrations of 3 to 30 mM; for A4V, the signal was more than five times that for the WT enzyme at an H_2O_2 concentration of 3 mM.
15. H. P. Misra, *J. Biol. Chem.* **254**, 11623 (1979).
16. D. A. Joyce, in *Variability in Response to Anti-Rheumatic Drugs*, P. M. Brooks, R. O. Day, G. G. Graham, K. M. Williams, Eds. (Birkhäuser, Basel, 1993), pp. 203–207.
17. Experiments were performed with conditions identical to those in Fig. 3, except that *d,l*-penicillamine was used in place of DDC. For both WT and A4V, the DMPO-OH signal was reduced by 60 to 95% in the presence of 13 μM penicillamine.
18. Both DDC and penicillamine inhibited the SOD activity of both WT and mutant CuZnSODs at high ratios of chelator to enzyme; however, the competing irreversible inhibition of CuZnSOD by H_2O_2 (*7*), the autooxidation of these sulfhydryl-containing Cu^{2+} chelators during the SOD assay, and the potential interference of these reagents with the assay itself (*24*) make conclusions concerning the concentrations required to inhibit the SOD activity of the enzymes and the mechanism of this activation uncertain (J. J. Goto, M. Wiedau-Pazos, E. B. Gralla, J. S. Valentine, unpublished data).
19. CSM14.1 is a conditionally immortalized rat nigral neural cell line [M. M. Durand, D. C. Chugani, M. Mahmoudi, M. E. Phelps, *Soc. Neurosci. Abstr.* **16**, 40 (1990); L. T. Zhong *et al.*, *Proc. Natl. Acad. Sci. U.S.A.* **90**, 4533 (1993)].
20. Studies with penicillamine and cultured CSM14.1 cells were performed as described for DDC. *d,l*-Penicillamine (100 or 500 μM) was added to the cultures at the time of serum withdrawal. Penicillamine had no significant effect on survival of cells transfected with the vector alone (control) or with the WT CuZnSOD construct. In contrast, addition of penicillamine to cells expressing A4V, G41D, or G85R mutant enzymes increased survival significantly. Cells expressing the G37R mutant showed a small penicillamine-induced improvement in survival, but this effect did not achieve statistical significance.
21. J. S. Beckman, M. Carson, C. D. Smith, W. H. Koppenol, *Nature* **364**, 584 (1993).
22. The mechanism proposed (*7–9*) for the WT bovine enzyme (Enz) is as follows:
$Enz\text{-}Cu(II) + H_2O_2 \rightarrow Enz\text{-}Cu(I) + O_2^- + 2H^+$
$Enz\text{-}Cu(I) + HO_2^- + H^+ \rightarrow Enz\text{-}Cu(II)(\cdot OH) + OH^-$
$Enz\text{-}Cu(II)(\cdot OH) + DMPO \rightarrow Enz\text{-}Cu(II) + DMPO\text{-}OH$
23. L. A. Damani, Ed., *Sulphur-Containing Drugs and Related Organic Compounds: Chemistry, Biochemistry, and Toxicology* (Halsted, New York, 1989), vol. 3B; D. R. Gandara *et al.*, *J. Clin. Oncol.* **13**, 490 (1995).
24. R. E. Heikkila and F. Cabbat, *Anal. Biochem.* **75**, 356 (1976).
25. G. R. Buettner and L. W. Oberley, *Biochem. Biophys. Res. Commun.* **83**, 69 (1978).
26. E. Finkelstein, G. M. Rosen, E. J. Rauckman, *Arch. Biochem. Biophys.* **200**, 1 (1980).
27. We thank C. J. Epstein and T.-T. Huang for the WT CuZnSOD genomic clone; D. R. Borchelt, P. C. Wong, and S. S. Sisodia for the mutant CuZnSOD genomic clones; R. H. Brown Jr., T. B. Usdin, M. J. Brownstein, and D. McKenna-Yasek for mutant CuZnSOD complementary DNAs; K. F. Faull for assistance with electrospray mass spectrometry; E. M. Landaw for assistance with statistical evaluation of the data; M. Durand and D. C. Chugani for CSM14.1 cells; J. Shi for technical assistance; and R. Y. N. Ho for technical advice. Supported by NIH grants AG12282 (D.E.B.), GM28222 (J.S.V.), and DK46828 (J.S.V.) and grants from the Amyotrophic Lateral Sclerosis Association (E.B.G.) and VivoRx Corp. (S.R.).

19 July 1995; accepted 27 November 1995

Identification of Scavenger Receptor SR-BI as a High Density Lipoprotein Receptor

Susan Acton,* Attilio Rigotti, Katherine T. Landschulz, Shangzhe Xu, Helen H. Hobbs, Monty Krieger†

High density lipoprotein (HDL) and low density lipoprotein (LDL) are cholesterol transport particles whose plasma concentrations are directly (LDL) and inversely (HDL) correlated with risk for atherosclerosis. LDL catabolism involves cellular uptake and degradation of the entire particle by a well-characterized receptor. HDL, in contrast, selectively delivers its cholesterol, but not protein, to cells by unknown receptors. Here it is shown that the class B scavenger receptor SR-BI is an HDL receptor. SR-BI binds HDL with high affinity, is expressed primarily in liver and nonplacental steroidogenic tissues, and mediates selective cholesterol uptake by a mechanism distinct from the classic LDL receptor pathway.

The risk of developing atherosclerosis, the leading cause of death in Western industrialized countries, is directly related to plasma concentrations of LDL cholesterol and inversely related to concentrations of HDL cholesterol (*1*, *2*). Although receptor-mediated LDL metabolism is well defined (*3*), HDL metabolism is poorly understood (*1*, *2*, *4*). HDL delivers cholesteryl ester to nonplacental steroidogenic tissues (ovary, adrenal gland, and testis) for hormone synthesis (*5*) and transports cholesterol from extrahepatic tissues to the liver (reverse cholesterol transport) (*1*, *2*, *4*). Unlike the situation with LDL, delivery of the cholesterol of HDL to cells is generally not accompanied by degradation of the protein component of HDL; this process is known as selective lipid uptake (*6–13*). Although numerous ligand-blotting studies revealed a variety of HDL-binding proteins [58 to 140 kD, reviewed in (*4*)], cell surface receptors for selective lipid uptake have not been identified. Here we provide evidence that the class B scavenger receptor SR-BI (*14*) is an HDL receptor.

We previously showed that hamster SR-BI (haSR-BI) binds native LDL, chemically modified LDL, and anionic phospholipids (*14*). To further explore the lipoprotein-binding properties and functions of SR-BI, we cloned the complementary DNA (cDNA) of the murine homolog (mSR-BI) and transfected it into ldlA cells [LDL receptor–negative Chinese hamster ovary (CHO) cells (*15*)]. ^{125}I-labeled HDL (*16*) specifically associated with the stable transfectants (ldlA[mSR-BI]) with high affinity (dissociation constant, K_d, of ~30 μg of protein per milliliter) and saturability (Fig. 1A). Control (untransfected) ldlA cells exhibited substantially less ^{125}I-HDL association. Association reached a steady state in less than 1 hour (Fig. 1B) and was not affected by EDTA [1 to 10 mM (*17*)] or by the removal of the trace amounts of apolipoprotein E (apoE) present in the HDL (*16*, *17*). There was little effect of excess native LDL on ^{125}I-HDL association (*17*); thus, LDL in vivo would not be expected to significantly interfere with binding of HDL to mSR-BI. The ^{125}I-labeled protein components of HDL (apoAI and apoAII) were not degraded [Fig. 1C and (*17*)], which is in marked contrast to the lysosomal degradation of the protein component of LDL (apoB) after endocytosis via the LDL receptor (*3*).

We next compared the fates of the protein (labeled with ^{125}I) and lipid [labeled with [^{3}H]cholesteryl oleate or DiI (a fluorescent lipid)] (*16*) components of HDL in mSR-BI–transfected cells. The amount of cell-associated ^{125}I-HDL reached a steady state in less than 1 hour at 37°C with less than 0.5% of the total label bound to the transfected cells (Fig. 2A). In contrast, transfer of [^{3}H]cholesteryl oleate and DiI increased continuously, reaching ~18% of the total labeled HDL lipids after 5 hours of incubation at 37°C. DiI accumulation was saturable (*17*). Untransfected cells displayed little lipid or protein association (Fig. 2B). Thus, there was selective transfer of the lipid, but not the protein, components of HDL to cells expressing mSR-BI. Essentially identical results were observed with COS cells transiently transfected (*14*) with either the mSR-BI vector or a control vector (pcDNA1, no insert) and incubated with HDL labeled with [^{3}H]cholesteryl ether or ^{125}I [10 μg of HDL protein per milliliter (*16*)]. After 5 hours, there was 18% lipid and 0.3% protein association in cells expressing mSR-BI and very little of either label associated with the controls.

S. Acton, A. Rigotti, S. Xu, M. Krieger, Department of Biology, Massachusetts Institute of Technology, Cambridge, MA 02139, USA.
K. T. Landschulz and H. H. Hobbs, Departments of Internal Medicine and Molecular Genetics, University of Texas Southwestern Medical Center, Dallas, TX 75235, USA.
*Present address: Millennium Pharmaceuticals, Cambridge, MA 02139, USA.
†To whom correspondence should be addressed.